THE YOUNG STELLAR POPULATION IN SERPENS AS OBSERVED BY ISOCAM*

A.A. Kaas[1], G. Olofsson[1], S. Bontemps[1,2], L. Nordh[1], M. Huldtgren[1], A. Abergel[3], P. André[4], F. Boulanger[3], M. Burgdorf[5], M.M. Casali[6], C.J. Cesarsky[4], E. Copet[7], E. Falgarone[8], T. Montmerle[4], M. Perault[8], P. Persi[9], T. Prusti[5], J.L. Puget[3], F. Sibille[10]

[1]Stockholm Observatory, Saltsjöbaden, Sweden
[2]Observatoire de Bordeaux, Floirac, France
[3]IAS, Université Paris XI, Orsay, France
[4]Service d'Astrophysique, CEA Saclay, Gif-sur-Yvette, France
[5]ISO Data Centre, ESA Astrophysics Division, Villafranca del Castillo, Spain.
[6]Royal Observatory, Blackford Hill, Edinburgh, UK
[7]DESPA, Obs. Paris-Meudon, Meudon, France
[8]ENS Radioastronomie, Paris, France
[9]IAS, CNR, Roma, Italy
[10]Observatoire de Lyon, France

ABSTRACT

We present the first results of a mid-IR survey of the star formation region in the Serpens Cloud. In total, 0.22 square degrees were mapped with ISOCAM in the two broad band filters LW2 (5 - 8.5 μm) and LW3 (12 - 18 μm), and fluxes were obtained for 550 and 210 point sources in LW2 and LW3, respectively. The colour index [14.3/6.7] was used to obtain a robust sample of YSOs. Among the 191 sources detected in both filters, 81 are identified as YSOs, of which only 28 where known from before. A lower limit of 400 YSOs per pc^2 is found for the densely clustered Cloud Core. The near-IR $J-H/H-K$ diagramme identifies only $\sim 1/3$ of the YSOs that are found by the single ISOCAM colour index [14.3/6.7]. We find that the Class I/Class II number ratio is large compared to other star formation regions, and this suggests that the Serpens Cloud contains an extremely young cluster. A preliminary luminosity function of the ISOCAM sample of Class II sources does not appear to turn over at the completeness limit of this survey.

Key words: ISO; Stars: formation; Stars: luminosity function; Stars: pre-main sequence; Infrared: stars

*ISO is an ESA project with instruments funded by ESA Member States (especially the PI countries: France, Germany, the Netherlands and the United Kingdom) and with the participation of ISAS and NASA.

1. INTRODUCTION

With the aim of deriving the IMF of a stellar cluster one can never overestimate the importance of extracting a complete sample of the cluster population. Young clusters are among the most desirable laboratories for IMF studies since they provide the most direct link between the stellar masses and the cloud structure from which they form. In addition, low mass objects are relatively luminous during their pre-main-sequence (PMS) evolution. Young clusters are, however, still embedded in their parent molecular clouds and the opacity of the dusty environment complicates the study of their members. The Serpens Cloud Core contains a compact, young cluster embedded in a clumpy, high-extinction cloud ($A_V \sim 50$) located only 5 degrees from the galactic plane at a distance of 259 ± 37 pc (Straižys et al. 1996). With the good sensitivity and spatial resolution of ISOCAM, we can study the cluster members at sufficiently long wavelengths to overcome most of the dust extinction. Sources with circumstellar dust observable as an intrinsic IR excess are certain YSOs. YSOs without IR excesses can not be distinguished from field stars, and additional data are required to obtain a full sample of the young stellar population.

Previous studies of the young stellar population in the near-IR (Eiroa & Casali 1992; Sogawa et al. 1997; Giovannetti et al. 1998) cover a small region only, and suffer from sample incompleteness if based on near-IR excesses alone, due to the high extinction. The present study in Serpens is a part of the ISO central programmes LNORDH.SURVEY_1 and GOLOFSSO.D_SURMC, which map nearby star formation regions with ISOCAM at 6.7 and 14.3 μm. See also Olofsson et al. (1999) and Bontemps et al. (1999).

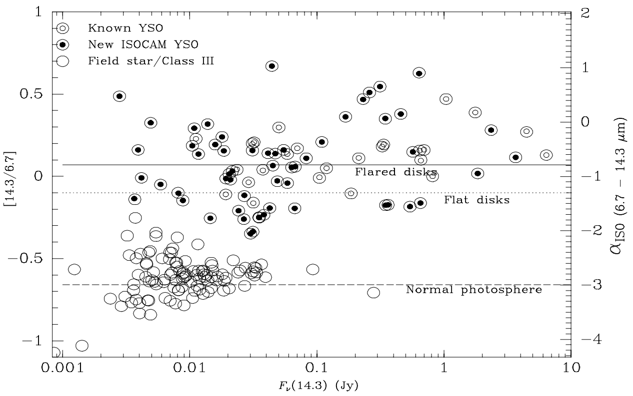

Figure 1. The colour index [14.3/6.7] *versus the flux at 14.3 μm in Jy. The index of the spectral energy distribution between 6.7 and 14.3 μm,* $\alpha_{\rm ISO}$*, is shown on the right y-axis. See text.*

2. OBSERVATIONS AND REDUCTIONS

In total, 0.22 square degrees were covered alltogether in LW2 and LW3 in 4 main rasters. The pixel field of view (PFOV) was 6 arcsec except for one region in LW2, where 3 arcsec was selected due to the risk of otherwise saturating the LW detector. Also in order to avoid saturation the intrinsic integration time was set to $T_{\rm int}$ = 0.28 s except for one field, where $T_{\rm int}$ = 2.1 s was used. Each position in the sky was observed during about 15 s. Three smaller and deeper rasters were made in selected subregions using PFOV = 3 arcsec, $T_{\rm int}$ = 2.1 s, staying about 90 s per sky position.

Each raster consists of a cube of frames which is reduced individually with the aid of the CIA[1] (CAM Interactive Analysis) package. The dark current was subtracted using the CAL-G dark from the ISOCAM calibration library and if necessary further improved by a second order dark correction using a FFT thresholding method. Cosmic ray hits were detected and masked by the multiresolution median transform (MMT) method (Starck et al. 1996). The transients in the time history of each pixel due to the slow response of the LW detector were treated with the IAS inversion method v.1.0 (Abergel et al. 1996). Flat-field images were constructed from the observations themselves. The imperfect correction for transients, as well as remains of cosmic ray glitches, complicate the source detection technique. We have developed an interactive IDL point source detection and photometry program for ISOCAM rasters which works within the CIA environment. Photometry of the detected point sources is measured on each individual coverage by aperture photometry. An aperture correction is made by use of the empirical point spread functions (PSFs) to insure that the flux lost in the broad wings is included, whatever the aperture size chosen. The fluxes in ADU/s in LW2 and LW3 are converted to mJy through the relations 2.19 and 1.96 ADU/s/mJy/pix for LW2 and LW3, respectively. No colour correction is made. The photometric uncertainty is about 20 %. See Kaas et al. (1999) for details.

[1]A joint development by the ESA Astrophysics Division and the ISOCAM Consortium led by the ISOCAM PI, C. Cesarsky, Direction des Sciences de la Matiere, C.E.A., France

3. RESULTS AND DISCUSSION

3.1. Identification of YSOs

Fluxes were obtained for 550 and 210 point sources in LW2 and LW3, respectively. The detection limits vary from raster to raster because of the different PFOVs and integration times, but typically, the 3 σ limit is 4 and 6 mJy for LW2 and LW3, respectively. 191 sources have reliable fluxes in both filters. For a small subregion centred on the Cloud Core near-IR photometry was obtained by deep $J(1.25\mu\rm m)$, $H(1.65\mu\rm m)$ and $K(2.2\mu\rm m)$ imaging with the ARcetri Near Infrared CAmera (ARNICA) mounted at the Nordic Optical Telescope (NOT) in 1996 (Kaas 1998). At a limiting magnitude of K = 19.0 practically all ISOCAM sources were detected also in K.

In Figure 1 the colour index [14.3/6.7], defined as $\log\{F_\nu(14.3\,\mu\rm m)/F_\nu(6.7\,\mu\rm m)\}$, is plotted against the flux at 14.3 μm. This colour index can be related to the spectral energy distribution (SED) index $\alpha = d\log(\lambda F_\lambda)/(d\log\lambda)$. An $\alpha_{\rm ISO}$ is calculated between 6.7 and 14.3 μm and indicated on the right y-axis. The sources separate into two distinct groups. For the first group the colour is that of normal photospheres, [14.3/6.7] = −0.69 or, equivalently, $\alpha_{\rm ISO} = -3$, as indicated with a dashed line. The spread around this value indicates the increasing photometric uncertainty with decreasing flux. The second group comprises all sources located well above the first group, i.e. sources with IR excess. This same dichotomy was found in the Chamaeleon dark clouds (Nordh et al. 1996) as well as in the ρ Ophiuchi cloud (Bontemps et al. 1999).

The fact that the intrinsic IR excess is so easily distinguished from reddening at these wavelengths enables us to reliably classify IR excess sources as young stellar objects (YSOs) on the basis of the single colour index [14.3/6.7]. We obtained a robust sample of 81 ISOCAM YSOs, of which only 28 were previously known. These sources have circumstellar dust, probably in the form of a disk. For reference, the predicted colours of flat and flared circumstellar disks (Kenyon & Hartmann 1995) are indicated in the figure as dotted and continuous lines, respectively.

Figure 2 shows the near-IR $J-H/H-K$ diagramme for 274 sources in a subregion centred on the Cloud Core (Kaas 1998). The loci of giant, supergiant and main-sequence stars are indicated with bold curves. The reddening line of an A0 star using the $A_\lambda \propto \lambda^{-1.7}$ extinction law is given as a dashed line (slope is 1.56) with every step of 10 A_V marked. Sources to the right of the reddening line have intrinsic excess in their $H-K$ colour due to the presence of circumstellar dust, and these are certain YSOs. The ISOCAM YSOs in this area are indicated with large

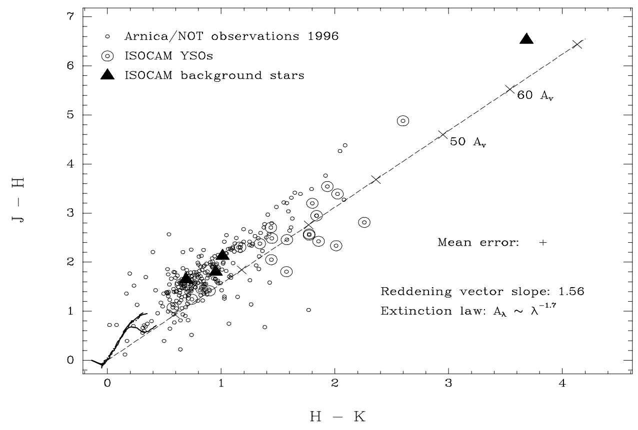

Figure 2. The standard near-IR colour diagramme for 274 sources in the central part of the Serpens Core, obtained from deep imaging with Arnica *at NOT.*

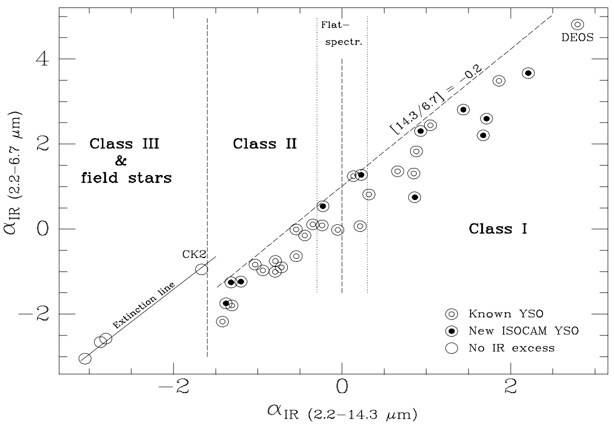

Figure 3. The spectral index $\alpha_{(2.2-6.7)}$ versus $\alpha_{(2.2-14.3)}$ for a subset of the ISOCAM sample. The location of Class I, Class II and Class III sources and field stars are indicated. Note the relatively large fraction of Class I sources in this diagramme.

circles. These are found to the left as well as to the right of the reddening line, however, and only 1/3 of these would be identified as IR-excess sources using the $J-H/H-K$ diagramme. This is probably due to a combination of 2 factors: the large influence from reddening in these bands, and the fact that circumstellar disks with inner holes do not exhibit near-IR excesses while they are expected to have excesses in the mid-IR. A sole use of the $J-H/H-K$ diagramme will systematically underestimate the IR-excess population, and might lead to severe sample incompleteness. Sources known from ISOCAM to be free of mid-IR excess are given as large filled triangles. There are only 4 such sources in this field, but their position in the diagramme are in good agreement with the extinction law applied for the near-IR.

3.2. Characterization of the YSOs in Serpens

Ground based K (2.2 μm) fluxes were combined with ISOCAM fluxes for the most active region of the Cloud Core, and the two indices $\alpha_{(2.2-14.3)}$ and $\alpha_{(2.2-6.7)}$ of the SED were calculated (see Figure 3). The index $\alpha_{(2.2-14.3)}$ is close to the α originally used by Lada (1987) to define 3 distinct classes of YSOs from the shape of their SED. Class I sources have $\alpha > 0$, a rising SED towards longer wavelengths, and are believed to be in an early evolutionary phase surrounded by a roughly spherical distribution of dust and gas. Class II sources are more evolved and have developed a disk-like distribution of the circumstellar dust. According to the revised scheme of André & Montmerle (1994), the boundary between Class II and Class III sources lies at $\alpha \approx -1.6$ and corresponds physically to the transition between optically thick and optically thin circumstellar disks. Figure 4 shows that our data agree better with $\alpha \approx -1.6$ than with the old $\alpha = -2$. While a few Class III sources are included (see Figure 1), the ISOCAM YSO sample is severly incomplete for this class of YSOs. Those without IR excesses can not be distinguished from field stars and are not included.

According to the $\alpha_{(2.2-14.3)}$ index, the number of Class I sources in the Cloud Core is of the order of the number of Class II sources. This is very unusual since Class II sources outnumber the Class I sources by typically 10 to 1 in star formation regions. The background supergiant CK2, seen through more than 60 A_V of extinction (see Figure 2), indicates an empirical slope of the extinction law, which is in agreement with the slope outlined by the group of mid-IR excess sources. Thus, in this sense, some of the sources classified as Class Is on the basis of Figure 3 could be highly extinguished Class II objects deeply embedded in the cloud. In order to disentangle the possible influence from local cloud extinction, Figure 4 shows $\alpha_{(6.7-14.3)}$ versus $\alpha_{(2.2-14.3)}$ for the same sources. Many of the above Class I sources are now located in the region where strongly reddened Class II sources are expected. Thus, constraining the definition of Class I sources by using the $\alpha_{(6.7-14.3)}$ index, which is less influenced by extinction, diminishes the Class I/Class II number ratio to about 1/3, which is still large compared to other star formation regions. Using $\alpha_{(6.7-14.3)}$ to constrain the total sample of 81 YSOs gives an average number ratio of 1/5 over the surveyed area. This strongly suggests that the Cloud Core is the youngest part of Serpens and perhaps the youngest among the nearby star formation regions. The mere existence of Class I sources suggests that star formation is going on in a rather continuous manner, and not in two separate phases as proposed by Casali et al. 1993 on the basis of near-IR and submm continuum data.

3.3. Luminosity function

Stellar luminosities ($L_\star$) are estimated for the 81 YSOs from the mid-IR fluxes, assuming that these are dominated by reprocessed stellar light by an optically thick, flat and passive circumstellar disk inclined at 60°. $L_\star$ obtained in this manner correlates

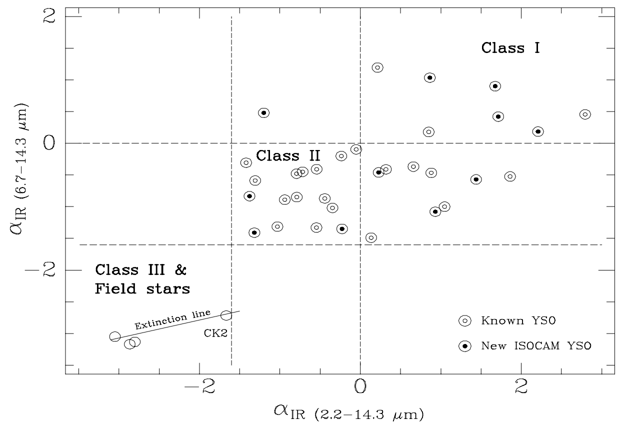

Figure 4. The index $\alpha_{(6.7-14.3)}$ versus $\alpha_{(2.2-14.3)}$ for a subset of the ISOCAM sample. The location of Class I, Class II and Class III sources and field stars as constrained by both indices are indicated.

well with that obtained from dereddened J band flux for the ρ Ophiuchi sample (Bontemps et al. 1999), although with some scatter. The luminosity function (LF) presented in Figure 5 is therefore referred to as preliminary. Error bars are from counting statistics only. Uncertainties in $L_\star$ are about a factor of 2 for Class II sources, and the binsize is set to $d\log L_\star = 0.5$. The fraction of Class I sources, as defined by the $\alpha_{(6.7-14.3)}$ index, is indicated with dotted bins. We anticipate that the Class I luminosities are underestimated, and that a major fraction of their total luminosities are radiated at longer wavelengths. An approximate completeness limit for excess sources at 14.3 μm is estimated to 16 mJy. This corresponds to about 0.12 $L_\odot$, leaving the two leftmost bins severly incomplete. Thus, the LF of the IR excess sources does not appear to turn over at low luminosities.

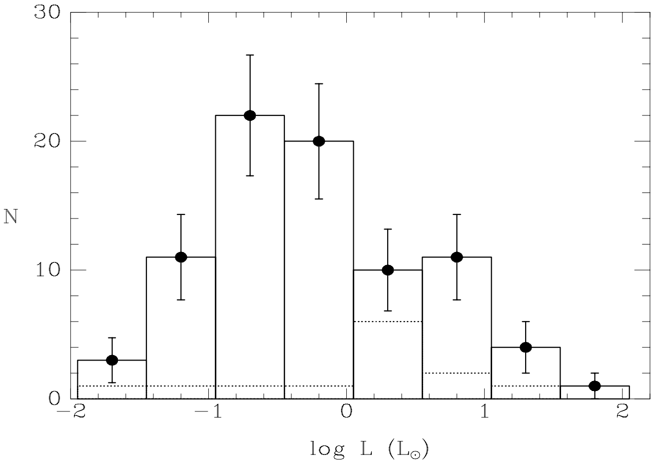

Figure 5. Preliminary luminosity function of the ISOCAM selected YSOs in Serpens. Dotted bars indicate the contribution of Class I sources.

The LF exhibits structure in the form of a peak at $\sim 6\,L_\odot$ and a dip around $2\,L_\odot$. Subtracting the Class I contribution (dotted bins), this structure becomes more apparent. Also, Figure 1 shows that there is a void of IR excess sources around 0.1 Jy in the 14.3 μm band. This does not necessarily imply that there is structure also in the IMF. Features in the LF could be due to e.g. the effect that deuterium burning has on the time-dependent LF (Zinnecker & McCaughrean 1991).

4. CONCLUSIONS

ISOCAM identified 81 YSOs with clear excesses in the [14.3/6.7] colour index, among which 65 % are new. A lower limit of 400 YSOs per pc^2 is found for the strongly clustered Cloud Core. The location of the ISOCAM YSOs in the standard near-IR $J-H/H-K$ diagramme demonstrates the limitation of the near-IR in extracting IR excess sources. For the first time we can characterize the IR excess sources in Serpens in terms of Class I and Class II sources. The unusually large number of Class Is in the Cloud Core could be an indication that this region is extremely young. Furthermore, the LF of the IR excess sources does not appear to turn over at the completeness limit of the survey.

REFERENCES

Abergel, A., Desert, F.-X., Aussel, H., 1996, "IAS model for ISOCAM LW transient correction"

André, P., Montmerle, T., 1994, ApJ, 420, 837

Bontemps, S., Nordh, L., Olofsson, G., et al. 1999, this volume

Casali, M.M., Eiroa, C., Duncan, W.D., 1993, A&A, 275, 195

Eiroa, C., Casali, M. M., 1992, A&A, 262, 486

Giovannetti, P., Caux, E., Nadeau, D., Monin, J.-L., 1998, A&A, 330, 990

Kaas, A.A., 1998, In: Astrophysics with the NOT, conf. proc., in press

Kaas, A.A., Bontemps, S., Olofsson, G., et al. 1999, in preparation for A&A

Kenyon, S.J., Hartmann, L., 1995, ApJS, 101, 117

Lada, C.J., 1987, In: IAU Symp. 115, Star Forming Regions, eds. Peimbert, M. & Jugaku, J., p. 1

Nordh, L., Olofsson, G., Abergel, A. et al. 1996, A&A, 315, L185

Olofsson, G., Kaas, A.A., Bontemps, S., et al. 1999, this volume

Sogawa H., Tamura M., Gatley I., Merrill K. M., 1997, AJ, 113, 1057

Starck J.L., Murtagh F., Pirenne B., Albrecht M., 1996, PASP, 108, 446

Straižys V., Černis K., Bartašiūtė S., 1996, Baltic Astronomy, 5, 125

Zinnecker, H., McCaughrean, M., 1991, Mem.S.A.It., 62, 761